JOURNAL OF Materials CHEMISTRY

Holographic gratings and holographic image storage *via* photochemical phase transitions of polymer azobenzene liquid-crystal films

Takahiro Yamamoto, Makoto Hasegawa, Akihiko Kanazawa, Takeshi Shiono and Tomiki Ikeda*

Research Laboratory of Resources Utilization, Tokyo Institute of Technology, 4259 Nagatsuta, Midori-ku, Yokohama, 226-8503, Japan. E-mail: tikeda@res.titech.ac.jp; URL: http://www.res.titech.ac.jp/polymer

Received 8th July 1999, Accepted 26th October 1999

Phase-type gratings formed by photochemical phase transitions of a polymer azobenzene liquid crystal have been characterized. The sensitivity of the material was improved by a factor of 23 in the liquid-crystalline phase owing to effective induction of the photochemical phase transition in the bright fringes of the interference pattern. A mechanism for grating formation in films based on dynamics both in grating formation and for the photochemical phase transition has been proposed. Observation of the grating structure with a polarizing optical microscope confirmed that the isotropic phase induced photochemically was arranged at well defined separations. The polymer azobenzene liquid crystal showed a storage capability of >100 Mbits cm^{-2} which corresponds to a resolution of <1 μm and a spatial frequency of >1000 lines mm^{-1}. We also attempted holographic image storage using a photomask as an object.

Introduction

In general, photosensitive materials used for holography should possess a number of specific characteristics: high diffraction efficiency, high resolution, environmental stability and high sensitivity. A variety of materials suitable for holography have been proposed and extensively investigated.[1–16] Use of polymeric materials for optical applications offers many advantages in comparison with the use of inorganic materials: low weight of optical components, good mechanical properties and ease in manufacturing technical parts even with a complex geometry. Below their glass transition temperature, segmental motion of polymer main chains is frozen-in. Therefore, a highly stable and rigid conformation is expected, which is favorable for information storage. In addition, such polymers enable formation of gratings with high spatial resolution. Combination of polymers with photochromic compounds such as azobenzene derivatives also provides high sensitivity, and photochromic polymers are expected to be among the most promising candidates as recording media for holograms. Indeed, Berg and coworkers recently introduced a new family of amorphous proline-based azobenzene peptides for holographic information storage.[3] They achieved fabrication of gratings showing high diffraction efficiency (80%) in thick films (*ca.* 13 μm). On the other hand, Wendorff and coworkers reported the formation of gratings with high diffraction efficiency (*ca.* 50%) and high spatial resolution (*ca.* 3000 lines mm^{-1}) by means of polymer liquid crystals (PLCs) containing azobenzene groups in the side chain.[5–8] In their study, the photoinduced change in birefringence was an order of 10^{-2} in thick films (*ca.* 7 μm), assuming that diffraction is caused by a change in refractive index alone.[6] They succeeded, for the first time, in storing holograms with PLCs at room temperature.[7] They also discussed the characteristics of the gratings theoretically in detail.[8] The advantage of liquid crystals lies in the fact that they show strongly anisotropic optical properties.

In a series of studies, we have demonstrated the formation of phase-type gratings based on photochemical nematic (N) to isotropic (I) phase transitions of various PLCs containing azobenzene moieties.[17–19] Isothermal N to I phase transitions were induced by photochemical reaction of the azobenzene moieties.[20–26] The photoinduced change in refractive index amounts to the order of 10^{-1} by this phase transition, which is obviously favorable for gratings with high diffraction efficiency and also for optical switching. We succeeded in rapid optical control of grating formation by switching writing beams in PLCs containing azobenzene moieties with strong electron-donating and electron-accepting groups at 4,4′-positions, in which the azobenzene moieties act simply as photoresponsive chromophores, to induce the thermal I to N phase transition effectively.[17,18] A large change in the refractive index (*ca.* 10^{-2}) was also induced in thin films (*ca.* 200 nm). It is known that some azobenzene derivatives show liquid-crystalline properties. Previously, we found a large enhancement of diffraction efficiency in phase-type gratings formed by the photochemical N to I phase transition of a polymer azobenzene LC in which azobenzene moieties act both as mesogens and photoresponsive chromophores.[19] This enhancement was attributed to spatial modulation of molecular alignments. Here, we present specific characteristics, such as stability of the stored information, spatial resolution and sensitivity, of this material. From dynamics both in grating formation and for photochemical phase transitions, we also propose a mechanism for the grating formation. On the basis of these results, we attempted holographic image storage in which an object can be reconstructed with irradiation of incoherent white light.

Experimental

Characterization of the polymer azobenzene LC

Fig. 1 shows the chemical structure of poly{6-[4-(4-ethoxyphenylazo)phenoxy]hexyl methacrylate} (**PM6AB2**) used in this study which was prepared and purified as previously reported.[27,28] Polymerization was conducted in *N,N*-dimethylformamide by the use of 2,2′-azobis(isobutyronitrile) as an initiator. The molecular weight of the polymer was determined

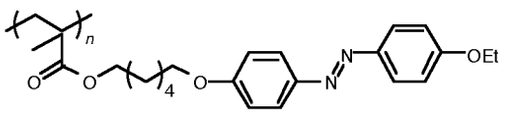

G 68 N 150 I
Mw = 78,000; Mw/Mn = 4.4
PM6AB2

Fig. 1 Chemical structure of **PM6AB2** used in this study. G, glass; N, nematic; I, isotropic; M_n, number-averaged molecular weight; M_w, weight-averaged molecular weight.

by gel permeation chromatography (GPC, Toyo Soda HLC-802; column, GMH6 X 2+G4000H8+G500H8; eluent, chloroform) calibrated with standard polystyrenes. Liquid-crystalline behavior and phase transition behavior were examined on a polarizing optical microscope (POM, Olympus, Model BH-2) equipped with Mettler hot-stage (Models FP-90 and FP-82). Thermotropic properties were determined with a differential scanning calorimeter (DSC, Seiko I&E, Models SSC-5200 and DSC220C) at a heating rate of 10 °C min^{-1}. At least three scans were performed to check the reproducibility. The thermodynamic properties and molecular weight of **PM6AB2** are given in Fig. 1 (Anal. Found: C, 70.39; H, 7.40; N, 6.84. Calc. for $C_{24}H_{30}N_4O_2$: C, 70.21; H, 7.38; N, 6.82%).

Film preparation and optical setup

In order to obtain a uniaxially aligned film, **PM6AB2** was dissolved in tetrahydrofuran (2 mg ml^{-1}) and then a small portion of the resultant solution was cast on a polyimide-coated glass substrate which had been rubbed unidirectionally. An optically transparent and homogeneously aligned film was obtained after annealing the film at a temperature just below the N to I phase transition temperature of **PM6AB2**. The thickness of the films was measured as 500–600 nm with a profile measurement microscope (Keyence, Model VF-7500).

Fig. 2 shows an object (A) and an optical setup (B) used for holographic image storage. This setup has been employed previously for recording of image holograms[29,30] and a similar setup was used in experiments related to grating formation. An Ar^+ laser (λ=488 nm; Laser Drive Inc., model 9600 for the laser power supply; National Laser Co., model H61WBLd0AW for the laser head) was employed as a light source of the writing beams in this study. Two beams of equal intensity obtained with a beam splitter were allowed to interfere on the film. The beams were depolarized and collimated to

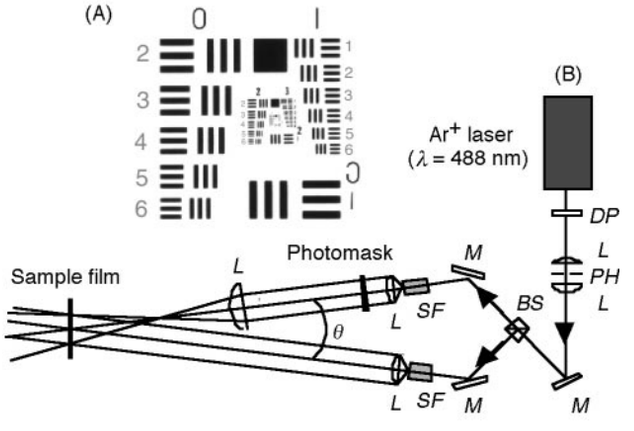

Fig. 2 Object (A) and optical setup (B) used for holographic image storage. The intensities of the object and the reference beams were adjusted at 1.1 and 1.6 mW cm^{-2}, respectively. The incident angle (2θ) of each writing beam was 14°. BS, beam splitter; DP, depolarizer; L, lens; M, mirror; PH, pinhole; SF, spatial filter.

diameters of *ca.* 2 and 30 mm for grating formation and image storage, respectively. The intensity of the writing beams was adjusted at 120 mW cm^{-2} for grating formation. In the holographic image storage, the intensities of the object and the reference beams were 1.1 and 1.6 mW cm^{-2}, respectively. The fringe spacing (Λ) was calculated by eqn. (1)

$$\Lambda = \lambda_w / 2 \sin\theta \quad (1)$$

where λ_w and θ are the wavelength and the incident angle of the writing beams, respectively. By changing θ from 6 to 20°, Λ was varied from 2.3 to 0.71 μm. Grating formation was evaluated by real-time monitoring of the change in intensity of a first-order diffraction beam at 633 nm from a He–Ne laser (NEC Co., Model GLS5360 for the laser power supply: GLG5260 for the laser head) as a readout beam. The readout beam was incident to the normal of the films. The propagation direction of the readout beam was opposite to that of the writing beams.

Evaluation of the photochemical N to I phase transition behavior of **PM6AB2** was performed by irradiation using a 488 nm unpolarized beam as a pumping beam. The intensity of a linearly polarized 633 nm probe beam, transmitted through a pair of crossed polarizers with the film between them, was monitored.

Characterization of gratings

First-order diffraction efficiency (η) is defined as the ratio of intensity of the first-order diffraction beam (I) to that of the incident beam (I_0) as expressed by eqn. (2)

$$\eta = I / I_0 \quad (2)$$

Photoinduced surface modulation was observed with an atomic force microscope (AFM, Seiko Instruments Inc. SPA-400 and SPI-3800N). Before and after exposure to two writing beams, the film was observed with polarized optical microscopy at room temperature.

Results and discussion

Sensitivity of the material

Fig. 3(A) and (B) show variation in the first-order diffraction efficiency as a function of exposure energy at 80 °C and room temperature, respectively. Multiple diffraction beams were immediately observed on irradiation of the writing beams at each temperature, since the grating formation was conducted in the Raman-Nath (thin) regime in this study. During exposure at 80 °C, the diffraction efficiency increased and reached a maximum value ($\eta \approx 20\%$) and then gradually decreased. On the other hand, no decay was observed when the film was exposed to the writing beams at room temperature and the diffraction efficiency was close to a saturated value η of 25%. Dashed lines in Fig. 3 indicate the exposure energy at which the gratings exhibited the same diffraction efficiency (η=20%). The exposure energy needed for η=20% was *ca.* 13 J cm^{-2} in the N phase and 300 J cm^{-2} in the glassy state. It is thus clear that effective formation of the grating was achieved in the N phase. In other words, the sensitivity of material was improved by a factor of 23 in the liquid-crystalline phase. In PLCs, the mobility of the mesogens in the liquid-crystalline phase is extremely high compared with that in the glassy state. Previously, we reported that the grating formation in polymer azobenzene LCs is associated with a photochemical phase transition: the photochemical phase transition of polymer azobenzene LCs proceeds even at room temperature and is induced readily in the liquid-crystalline phase.[19] It is, therefore, reasonable to consider that this improvement in the sensitivity is attributed to an effective induction of the photochemical phase transition which occurred in bright fringes of interference pattern. Evaluation of photoinduced surface modulation by

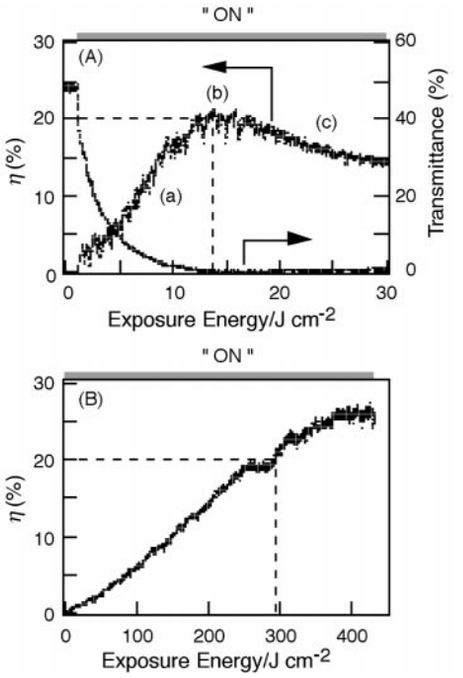

Fig. 3 First-order diffraction efficiency (η) as a function of exposure energy at 80 °C (A) and room temperature (B). The total intensity of the writing beams was 120 mW cm^{-2} in both cases. Incident angle (θ) of each writing beam was 7° which corresponds to a resolution of 2 μm. The dashed lines indicate an exposure energy required for $\eta = 20\%$. (A) also shows the change in transmittance upon the photochemical phase transition of **PM6AB2**. The intensity of the pump beam was 120 mW cm^{-2}.

AFM also demonstrated that grating formation was effective in the N phase. Fig. 4 and 5 show three-dimensional and slice view of AFM images which were recorded at 80 °C and room temperature, respectively. Both gratings showed almost the same diffraction efficiency ($\eta \approx 20\%$), however, when grating formation was conducted in the N phase, a grating with $\eta \approx 20\%$ was obtained only with a slight modulation of the surface structure.

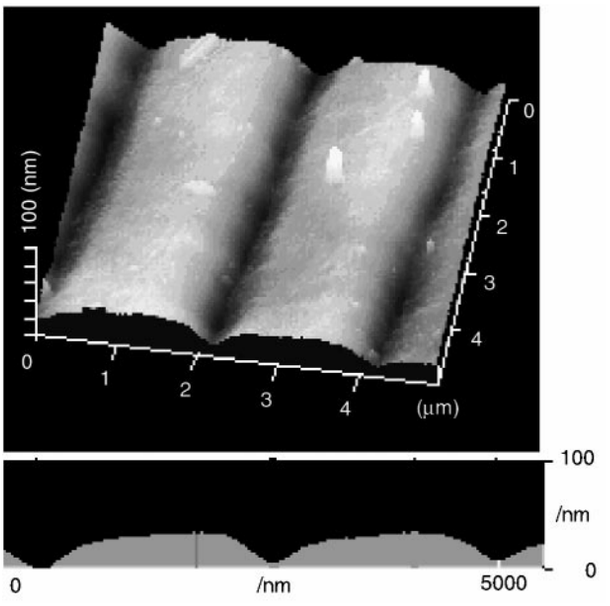

Fig. 4 AFM three-dimensional and slice views of the grating recorded at 80 °C (N phase). This grating showed $\eta \approx 20\%$ with a surface modulation of *ca.* 30 nm. The AFM measurement was conducted at room temperature.

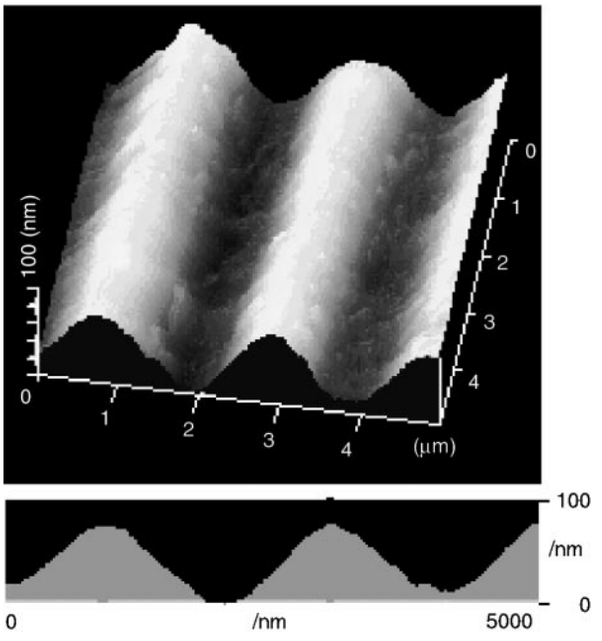

Fig. 5 AFM three-dimensional and slice views of the grating recorded at room temperature (glassy state). This grating showed $\eta \approx 20\%$ with a surface modulation of *ca.* 70 nm. The AFM measurement was conducted at room temperature.

Mechanism for grating formation

Fig. 3(A) also shows the change in transmittance due to the photochemical phase transition of **PM6AB2**. An unpolarized 488 nm beam from the Ar^+ laser was employed as the pumping beam. The transmittance of the probe beam gradually decreased on irradiation of the pumping beam which caused *trans–cis* photoisomerization of azobenzene moieties. From dynamics both of the grating formation and of the photochemical phase transition, we can speculate that the formation of a grating in the film consists of three processes [(a), (b) and (c) as shown in Fig. 3(A)]. Mechanisms for the generation of relief-structures on polymer films have been extensively discussed by Natansohn and coworkers[13,14] Here, the mechanism for grating formation in the film is schematically illustrated in Fig. 6 where processes (a), (b) and (c) in Fig. 3(A) correspond to (a), (b) and (c) in Fig. 6, respectively. In process (a), *trans–cis* photoisomerization generates small I domains in bright fringes of the pattern, which grow on further irradiation. If the refractive indices of the N and the I phases are n and n', respectively, the difference in the refractive index (Δn) between n (the dark fringes) and n' (the bright fringes) becomes larger during exposure as the photochemical phase transition proceeds. Hence, the diffraction efficiency increases. In process (b), the diffraction efficiency reaches a maximum value, indicating that the photochemical phase transition is complete in the bright fringes and Δn reaches a maximum. Further irradiation of the writing beams leads to a decay of the diffraction efficiency [process (c)] causing a reduction of Δn. In this process, the orientational order of the azobenzene moieties decreases in the dark fringes of the pattern. Two factors may be responsible for the decrease. One is induction of the photochemical phase transition in the dark fringes. Since the light intensity on the film is sinusoidal, photochemical reaction may occur even in the 'dark' fringes, so that the photochemical phase transition occurs gradually in the boundary between the dark and the bright fringes of the pattern. Propagation of perturbation of the phase transition to the dark fringes may also occur[17] which induces a decrease of the orientational order of the azobenzene moieties in the dark fringes.

To confirm our assumption, we observed gratings directly with polarized optical microscopy. Fig. 7 shows the photo-

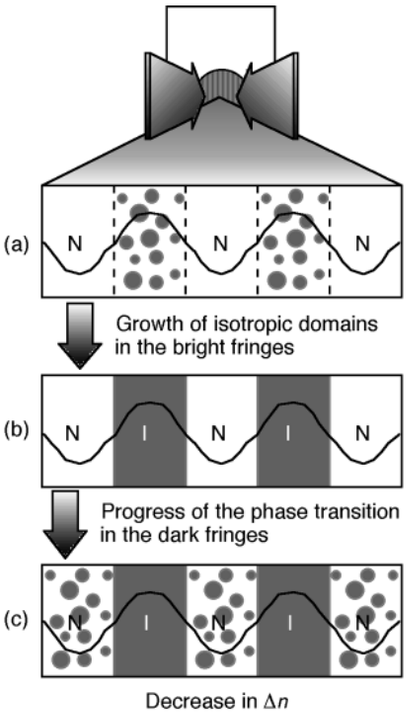

Fig. 6 Plausible mechanism for the formation of a grating in the **PM6AB2** film. States (a), (b) and (c) correspond to processes shown in Fig. 3(A). (a): generation and growth of the isotropic domains in bright fringes of interference pattern; (b): complete induction of the photochemical phase transition in bright fringes; (c): induction of the photochemical phase transition in dark fringes.

graphs of the film before (A), and after (B), exposure to the writing beams. The grating formation was conducted at $\theta = 7^\circ$ which corresponds to a resolution of 2 μm. Before exposure to the writing beams, the film was observed to be bright with no structural features through crossed polarizers in POM [Fig. 7(A)] as a consequence of homogeneous alignment of the azobenzene moieties in the film. However, as shown in Fig. 7(B), a fringe structure composed of bright and dark regions was observed after exposure. The fringe spacing as confirmed by AFM measurements was *ca.* 2 μm is in good agreement with the theoretically estimated value. In the bright regions, the N phase was preserved, while in the dark regions birefringence disappeared after exposure to the writing beams. It is clear that the I phases induced by the photochemical phase transition of **PM6AB2** are arranged at well defined separations.

Thermal stability of the stored information

Fig. 8 shows changes in the first-order diffraction efficiency after interruption of exposure at different temperatures. When the highest diffraction efficiency was observed at each temperature, the writing beams were switched off. An increase in the diffraction efficiency was observed at all temperatures when the writing beams were turned off as shown in Fig. 8. This increase is attributed either to retrieval of the N phase (thermal I to N phase transition) in the dark fringes or to growth of relief-structure in the bright fringes of the interference pattern. In the formation of gratings, these would contribute to an increase in the diffraction efficiency, since the efficiency is a function of modulations in refractive index and surface structure. Although the real-time monitoring of growth of the relief-structure is very difficult, the thermal I to N phase transition behavior at given temperatures can be readily evaluated as shown in Fig. 9. It was clearly observed that a small birefringence was recovered when the pumping beam was turned off. We reported previously that the rate-determining step for the I to N phase transition is a *cis–trans*

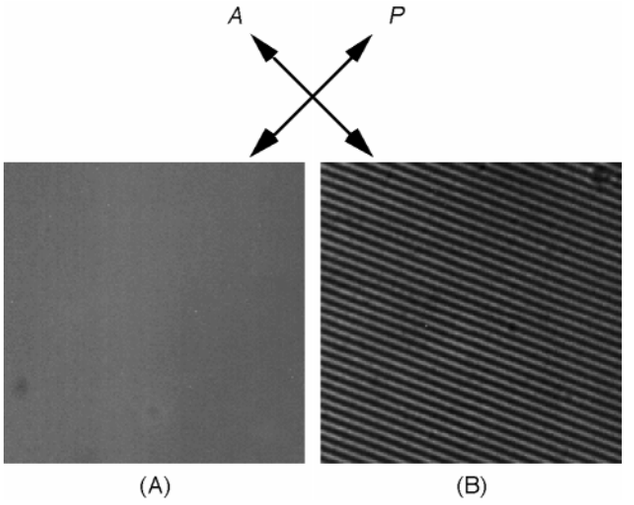

Fig. 7 Observation of the **PM6AB2** film before (A) and after (B) grating formation. The film was viewed through crossed polarizers in a polarizing optical microscope. The grating formation was performed at $\theta = 7^\circ$ which corresponds to a resolution of 2 μm. A, analyzer; P, polarizer.

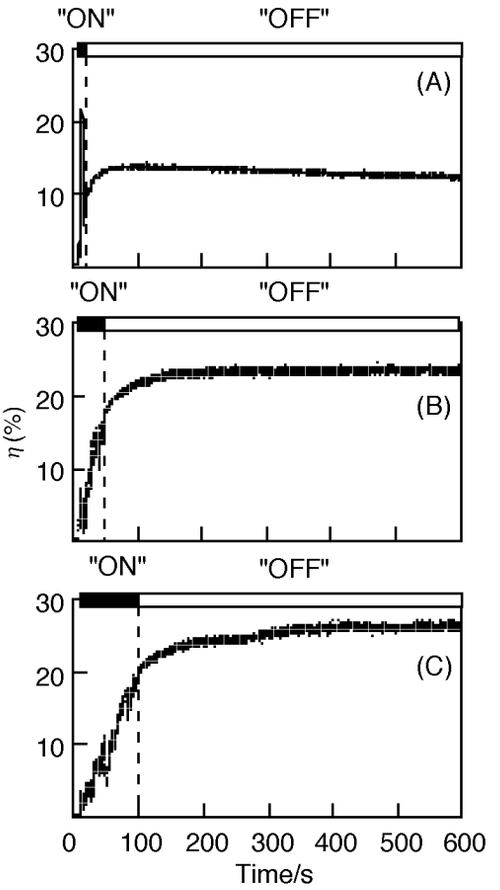

Fig. 8 Thermal stability of the recorded gratings at various temperatures. When the diffraction efficiency reached an approximately maximum value at each temperature, writing beams were turned off: (A) 100, (B) 90 and (C) 80 °C.

back isomerization process of the azobenzene moiety.[21] *cis–trans* Isomerization proceeded even at room temperature and took place quite effectively at $>100\,^\circ$C.[20] Although the effect of growth of relief-structure is important, a small recovery of birefringence in the dark fringes would also partly be responsible for the increase in the efficiency.

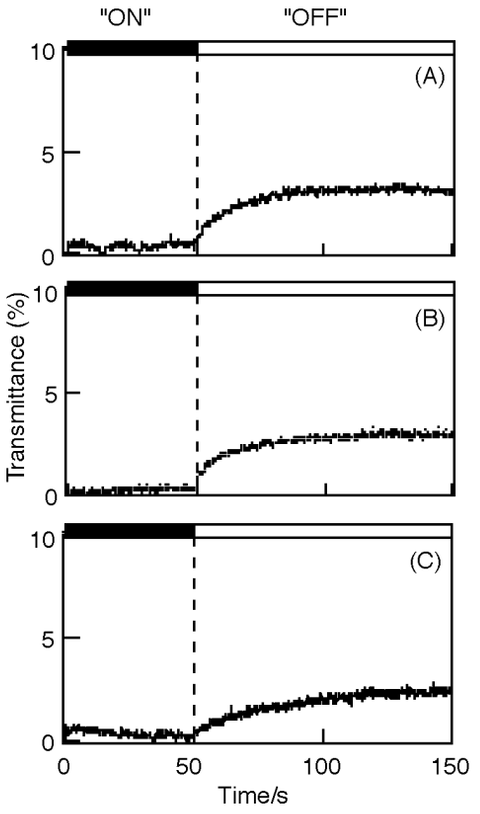

Fig. 9 Thermal I to N phase transition behavior at various temperatures [(A) 100, (B) 90 and (C) 80 °C].

On the other hand, no significant decay in the diffraction efficiency was observed after the writing beams were turned off at all temperatures studied (Fig. 8) which indicates that the gratings show high thermal stability. As is apparent from Fig. 9, complete induction of the thermal I to N phase transition was not observed over our time scale. Therefore, the high thermal stability of the stored information is due to an only slow restoring of the N phase at bright fringes. At present, more detailed studies related to increase in the diffraction efficiency and thermal stability of the gratings are in progress.

Spatial resolution and storage capability

In practical uses, resolution and storage capability of materials are very important factors. With this in mind we investigated the first-order diffraction efficiency as a function of spatial frequency and results are shown in Fig. 10. The incident angle (θ) of each writing beam was varied from 6 to 20°, leading to a change in the fringe spacing (spatial resolution) from 2.3 to 0.71 μm which corresponds to a spatial frequency change from 430 to 1400 lines mm^{-1}. The diffraction efficiency showed a maximum value (>20 %) at 500 lines mm^{-1} in the thin film. It is interesting that efficiencies of several percent were observed for a wide range of spatial frequencies up to 1000 lines mm^{-1} which corresponds to a resolution of 1 μm or a storage capability of 100 Mbits cm^{-2}. Given that a spatial frequency of at least 1000 lines mm^{-1} is required for holographic image storage, **PM6AB2** would appear to be suitable for holographic image storage. In polymeric systems, mobility of mesogens is suppressed relative to that in low-molecular-weight LCs, since the mesogens are covalently bonded to the main chains of the polymer and formation of gratings with high spatial frequency can thus result. Values of the spatial frequency can be improved by suppression of mobility of mesogens as well as optimization of the experimental conditions. Other research groups have also reported gratings with a high spatial frequency.[1,2,7,8]

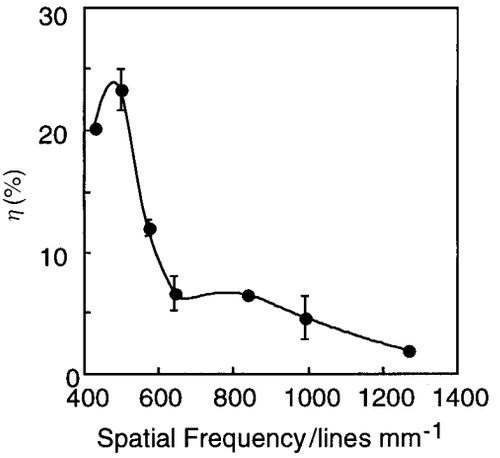

Fig. 10 First-order diffraction efficiency as a function of spatial frequency. The incident angle (θ) of each writing beam was varied from 6 to 20°, leading to a change in the spatial frequency from 430 to 1400 lines mm^{-1}. Grating formation was conducted at 80 °C and the total intensity of the writing beams was 120 mW cm^{-2}.

Holographic image storage

Based on these results, we attempted holographic image storage in **PM6AB2** films and the optical setup used is shown in Fig. 2(B). This setup has been employed previously for recording of Fourier transform holograms (image hologram).[29,30] The most significant advantage of this method is that a small angular deviation does not affect reconstruction. Thus, large, wide-band reconstruction light sources can be used,[28] and reconstructed images can be observed by irradiation even with incoherent white light. We employed a photomask shown in Fig. 2(A) as an object. In this study, the image storage was conducted at room temperature. The intensities of the object and the reference beams were 1.1 and 1.6 mW cm^{-2}, respectively, the exposure time was 120 min and the exposure energy was 19.5 J cm^{-2}. Fig. 11 shows the reconstructed images obtained upon irradiation with white light and it was evident that the object was reconstructed with a relatively high resolution. The color of the image differed when

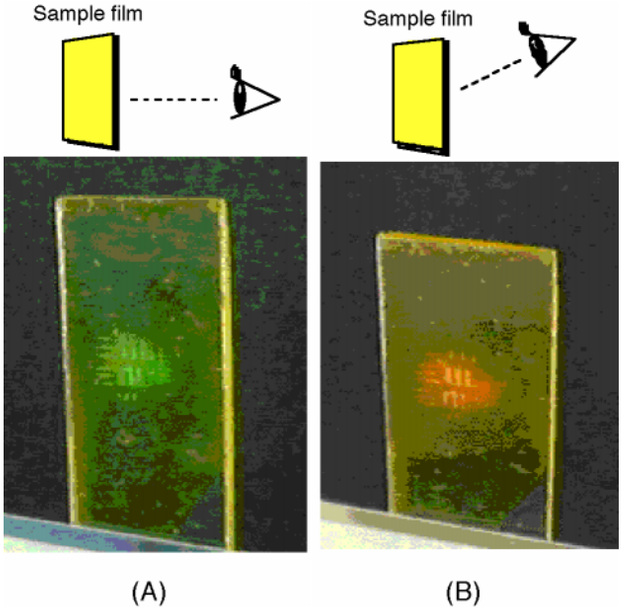

Fig. 11 Reconstructed images observed at side (A) and diagonal (B) positions. Reconstruction was performed by irradiation with incoherent white light at room temperature. Holographic image storage was carried out at room temperature and the exposure time was 120 min (exposure energy *ca.* 19.5 J cm^{-2}).

the film was viewed at different angles, from side (A) and diagonal (B) positions. This fact clearly indicates that the holographic diffraction grating was formed in the film, rather than the focused image of the object being stored directly. The stored image remained unchanged after 12 months.

Conclusion

Several characteristics, such as sensitivity, thermal stability of the stored information, resolution and storage capability, and holographic image storage have been examined with polymer azobenzene LC films. It was found that the polymer azobenzene LC shows a relatively high performance as a holographic recording medium. The sensitivity of the material was improved in the N phase due to an effective induction of the photochemical phase transition in the bright fringes of the interference pattern. The stored grating was highly stable in the LC phase as well as in the glassy state. This was a consequence of the slow thermal I to N phase transition. Holographic image storage of a photomask was achieved and the object could be reconstructed clearly by irradiation even with incoherent white light.

References

1 S. Hvilsted, F. Andruzzi and P. S. Ramanujam, *Opt. Lett.*, 1992, **17**, 1234.
2 S. Hvilsted, F. Andruzzi, C. Kulinna, H. W. Siesler and P. S. Ramanujam, *Macromolecules*, 1995, **28**, 2172.
3 P. H. Rasmussen, P. S. Ramanujam, S. Hvilsted and R. H. Berg, *J. Am. Chem. Soc.*, 1999, **121**, 4738.
4 L. Andruzzi, A. Altomare, F. Ciardelli, R. Solaro, S. Hvilsted and P. S. Ramanujam, *Macromolecules*, 1999, **32**, 448.
5 M. Eich, B. Reck, H. Ringsdorf and J. H. Wendorff, *Proc. SPIE-Int. Soc. Opt. Eng.*, 1986, **682**, 93.
6 M. Eich and J. H. Wendorff, *Makromol. Chem., Rapid Commun.*, 1987, **8**, 59.
7 M. Eich and J. H. Wendorff, *Makromol. Chem., Rapid Commun.*, 1987, **8**, 467.
8 M. Eich and J. H. Wendorff, *J. Opt. Soc. Am. B*, 1990, **7**, 1428.
9 B. K. Mandal, R. J. Jeng, J. Kumar and S. K. Tripathy, *Makromol. Chem., Rapid Commun.*, 1991, **12**, 607.
10 D. Y. Kim, S. K. Tripathy, L. Li and J. Kumar, *Appl. Phys. Lett.*, 1995, **66**, 1166.
11 D. Y. Kim, L. Li, X. L. Jiang, V. Shivshankar, J. Kumar and S. K. Tripathy, *Macromolecules*, 1995, **28**, 8835.
12 T. S. Lee, D. Y. Kim, X. L. Jiang, L. Li, J. Kumar and S. K. Tripathy, *J. Polym. Sci. A: Polym. Chem.*, 1998, **36**, 283.
13 P. Rochon, E. Batalla and A. Natansohn, *Appl. Phys. Lett.*, 1995, **66**, 136.
14 C. J. Barrett, A. Natansohn and P. L. Rochon, *J. Phys. Chem. B*, 1996, **100**, 8836.
15 J. Contzen, G. Heppke, H.-S. Kitzerow, D. Krüerke and H. Schmid, *Appl. Phys. B*, 1996, **63**, 605.
16 H. J. Eichler, R. Elschner, R. Macdonald, G. Heppke and H. Schmid, *Mol. Cryst. Liq. Cryst.*, 1994, **250**, 293.
17 M. Hasegawa, T. Yamamoto, A. Kanazawa, T. Shiono and T. Ikeda, *Adv. Mater.*, 1999, **11**, 675.
18 M. Hasegawa, T. Yamamoto, A. Kanazawa, T. Shiono and T. Ikeda, *Chem. Mater.*, 1999, **11**, 2764.
19 T. Yamamoto, M. Hasegawa, A. Kanazawa, T. Shiono and T. Ikeda, *J. Phys. Chem. B*, 1999, **103**, 9873.
20 T. Ikeda and O. Tsutsumi, *Science*, 1995, **268**, 1873.
21 O. Tsutsumi, T. Shiono, T. Ikeda and G. Galli, *J. Phys. Chem. B*, 1997, **101**, 1332.
22 O. Tsutsumi, T. Kitsunai, A. Kanazawa, T. Shiono and T. Ikeda, *Macromolecules*, 1998, **31**, 355.
23 O. Tsutsumi, Y. Demachi, A. Kanazawa, T. Shiono, T. Ikeda and Y. Nagase, *J. Phys. Chem. B*, 1998, **102**, 2869.
24 A. Shishido, O. Tsutsumi, A. Kanazawa, T. Shiono, T. Ikeda and N. Tamai, *J. Am. Chem. Soc.*, 1997, **119**, 7791.
25 A. Shishido, O. Tsutsumi, A. Kanazawa, T. Shiono, T. Ikeda and N. Tamai, *J. Phys. Chem. B*, 1997, **101**, 2806.
26 H.-K. Lee, A. Kanazawa, T. Shiono, T. Ikeda, T. Fujisawa, M. Aizawa and B. Lee, *Chem. Mater.*, 1998, **10**, 1402.
27 A. S. Angeloni, D. Caretti, C. Carlini, G. Chiellini, G. Galli and A. Altomare, *Liq. Cryst.*, 1989, **4**, 513.
28 H. Ringsdorf and H. W. Shmidt, *Makromol. Chem.*, 1984, **185**, 1327.
29 R. J. Collier, C. B. Burckhardt and L. H. Lin, *in Optical Holography*, Academic Press, New York, 1971, p. 204.
30 L. Rosen, *Appl. Phys. Lett.*, 1966, **6**, 337.

Paper a905501k